Dynamin2- and endothelial nitric oxide synthase–regulated invasion of bladder epithelial cells by uropathogenic *Escherichia coli*

Zhimin Wang,[1,4,5] Ceba Humphrey,[1] Nicole Frilot,[1] Gaofeng Wang,[3] Zhongzhen Nie,[1,4,5] Nader H. Moniri,[2] and Yehia Daaka[1,4,5]

[1]Department of Pathology, Medical College of Georgia, Augusta, GA 30912
[2]Department of Pharmaceutical Sciences, College of Pharmacy and Health Sciences, Mercer University, Atlanta, GA 30341
[3]John P. Hussman Institute for Human Genomics, University of Miami Miller School of Medicine, Miami, FL 33136
[4]Department of Urology and [5]Prostate Disease Center, University of Florida, Gainesville, FL 32610

Invasion of bladder epithelial cells by uropathogenic *Escherichia coli* (UPEC) contributes to antibiotic-resistant and recurrent urinary tract infections (UTIs), but this process is incompletely understood. In this paper, we provide evidence that the large guanosine triphosphatase dynamin2 and its partner, endothelial nitric oxide (NO) synthase (NOS [eNOS]), mediate bacterial entry. Overexpression of dynamin2 or treatment with the NO donor S-nitrosothiols increases, whereas targeted reduction of endogenous dynamin2 or eNOS expression with ribonucleic acid interference impairs, bacterial invasion. Exposure of mouse bladder to small molecule NOS inhibitors abrogates infection of the uroepithelium by *E. coli*, and, concordantly, bacteria more efficiently invade uroepithelia isolated from wild-type compared with eNOS$^{-/-}$ mice. *E. coli* internalization promotes rapid phosphorylation of host cell eNOS and NO generation, and dynamin2 S-nitrosylation, a posttranslational modification required for the bacterial entry, also increases during *E. coli* invasion. These findings suggest that UPEC escape urinary flushing and immune cell surveillance by means of eNOS-dependent dynamin2 S-nitrosylation and invasion of host cells to cause recurrent UTIs.

Introduction

Urinary tract infections (UTIs) are among the most common serious pathogenic infections in the Western world. UTIs affect a broad demographic, including infants, children, and the elderly, but women are at higher risk, nearly 40 times higher than men, for acquiring the disease (Foxman et al., 2000). It is estimated that a third of all women with UTIs have recurrent infections within the first 6 mo after initial antibiotic treatment. Although multiple uropathogens have been implicated as causative agents, >80% of UTIs are caused by *Escherichia coli* expressing filamentous adhesion units termed type I fimbriae (Johnson, 1991). These fimbriae are thought to initiate chronic UTIs by mediating the adherence of *E. coli* to the bladder epithelium, and available evidence suggests that fimbriae-mediated adherence can be followed by invasion of the bacterium into the urothelium (Connell et al., 1996; Mulvey et al., 2001; Dhakal et al., 2008). This intracellular invasion presumably leads to a quiescent infection, in which the intracellular bacteria are inaccessible to host immune cells or cell-impermeable antibiotics. The invasive nature of these infections may explain, at least in part, the frequent reoccurrence of UTIs and the greater incidence of antibiotic resistance.

Emerging evidence implicates the cell membrane–associated endocytotic machinery in the invasion (entry) of bacteria into the host cell (Mulvey, 2002; Dhakal et al., 2008). This cellular machinery, typically involved in endocytosis of membrane-bound receptors or other membrane components, may include cavelike lipid rafts (e.g., caveolae) and clathrin-coated pits.

Correspondence to Yehia Daaka: ydaaka@ufl.edu

Abbreviations used in this paper: ANOVA, analysis of variance; BEC, bladder epithelial cell; eNOS, endothelial NOS; GAPDH, glyceraldehyde 3-phosphate dehydrogenase; iNOS, inducible NOS; MβCD, methyl-β-cyclodextrin; nNOS, neuronal NOS; NO, nitric oxide; NOS, NO synthase; shRNA, small hairpin RNA; UPEC, uropathogenic *Escherichia coli*; UTI, urinary tract infection.

The Rockefeller University Press $30.00
J. Cell Biol. Vol. 192 No. 1 101–110
www.jcb.org/cgi/doi/10.1083/jcb.201003027

Significantly, both caveolae- and clathrin-coated pit–based fission from the plasma membrane have been shown to be dependent on the enzymatic activity of large GTPase dynamin proteins, such as dynamin2, a multidomain GTPase that catalyzes budding of endocytotic vesicles (Conner and Schmid, 2003; Doherty and McMahon, 2009; Mettlen et al., 2009). Dynamin2 has been shown to be directly involved in the internalization of viral pathogens, and the internalization of several viruses, including HIV, is inhibited when a dominant-negative form (K44A) is expressed (Pizzato et al., 2007) or when dynamin function is inhibited (Miyauchi et al., 2009). During the late stages of vesicle formation, dynamin self-assembles into rings that encircle the neck of the invaginated membrane. Although the exact mechanism of dynamin-mediated fission is still debated (Conner and Schmid, 2003), it is well established that the self-assembly of protein monomers regulates GTP hydrolysis, facilitating the detachment of the invaginated neck and yielding an endocytotic vesicle.

The ability of dynamin to mediate fission of cargo-containing invaginated pits from the plasma membrane is partially regulated by interactions with partner lipids and proteins. For example, the central pleckstrin homology domain binds phosphoinositides and other proteins leading to dynamin recruitment to the plasma membrane (Achiriloaie et al., 1999). The proline- and arginine-rich carboxy terminus binds several proteins, including c-Src, which phosphorylates dynamin to enable active receptor-mediated endocytosis (Ahn et al., 1999). Endothelial nitric oxide (NO) synthase (NOS [eNOS]) is another dynamin2-interacting protein (Cao et al., 2001), and we recently showed that ectopically overexpressed neuronal dynamin1 and neuronal NOS (nNOS) proteins in model HEK293 cells form a complex that regulates vesicle trafficking from the plasma membrane (Wang et al., 2006).

Uropathogenic *E. coli* (UPEC), the causative agents of the vast majority of UTIs (Johnson, 1991), invade host bladder epithelial cells (BECs) using a stepwise process that involves the binding of bacterial type I fimbriae (Connell et al., 1996; Mulvey et al., 2001) to specific host cell plasma membrane receptors (Krogfelt et al., 1990), formation of membrane invaginations, and fission of the budding vesicles containing UPEC into the cytosol (Duncan et al., 2004; Bishop et al., 2007). Physical transport of the UPEC from the extracellular milieu to inside the cell can be monitored with microscopic imaging, but knowledge at the molecular level, which is required for a targeted pharmacological approach, remains incompletely understood. Here, we use BECs and intact mouse bladders in bacterial infection assays to show that endogenous dynamin2 regulates UPEC invasion via a mechanism that involves eNOS-mediated dynamin2 S-nitrosylation.

Results

Dynamin2 regulates the UPEC invasion

We used the laboratory reference *E. coli* ORN103(pSH2) strain that expresses type 1 fimbriae and has been demonstrated to recapitulate the UPEC invasion (Mulvey et al., 2001; Bishop et al., 2007) and the cholesterol-sequestering, caveolae-disrupting agent methyl-β-cyclodextrin (MβCD) in previously described gentamicin protection assays (Duncan et al., 2004) to verify that bacterial invasion occurs through plasma membrane lipid-rich vesicle portals. The MβCD dose-dependently reduced the *E. coli* ORN103(pSH2) invasion, and the addition of cholesterol after MβCD treatment fully restored the invasive capability (Fig. S1 A), which was consistent with the conclusion that intracellular invasion of UPEC into BECs is mediated, at least in part, by caveolar portals (Duncan et al., 2004).

The large GTPase dynamin plays a central role in endocytic budding of vesicles from the plasma membrane (Conner and Schmid, 2003), suggesting a role for dynamin in the bacterial entry into host BECs. Accordingly, forced overexpression of ubiquitously expressed dynamin2 significantly increased the number of intracellular bacteria when compared with mock-transfected controls, and, reciprocally, the overexpression of GTPase-deficient dominant-negative dynamin2 K44A decreased the *E. coli* ORN103(pSH2) invasion of BECs (Fig. 1 A). These results are supported by recent findings showing that inhibition of dynamin function with small molecule dynasore impairs bacterial invasion (Veiga et al., 2007; Eto et al., 2008). To discount the possibility that dynamin2 was involved in nonspecific modulation of bacterial internalization, such as increasing adherence, we performed the invasion assay at 4°C, a condition that is not permissive for vesicle trafficking from the plasma membrane into the cytosol. The results show that forced overexpression of either wild-type or K44A forms of dynamin2 does not impact the bacterial binding to BECs (Fig. S1 B). To further confirm that dynamin2 specifically affects endocytotic entry, we assessed the effects of overexpressing wild-type and K44A forms of dynamin2 on the entry of *Salmonella typhimurium*, a pathogen that invades cells through macropinocytosis (Francis et al., 1993; Pizarro-Cerdá and Cossart, 2006), a dynamin2-independent process. Results show that *S. typhimurium* entry into BECs is unaffected by the forced overexpression of wild-type or K44A forms of dynamin2 (Fig. S1 C), reinforcing the idea that dynamin2-mediated vesicle trafficking is used during invasion from the plasma membrane.

To directly implicate the exploitation of host BEC dynamin2 during the UPEC invasion, we modulated endogenous dynamin2 expression with small hairpin RNA (shRNA) and used clinical UPEC isolates. We used three commercially obtained lentiviruses that express dynamin2-specific shRNA (Dyn2shRNA) or a control shRNA that targets GFP (GFP-shRNA). Immunoblotting of cell lysates indicated a >80% reduction in dynamin2 protein levels by Dyn2shRNA in comparison with GFPshRNA (Fig. S1 D). The stable dynamin2 knockdown BEC line D2-6649 was used to confirm the function of dynamin2 in the UPEC invasion. Bacterial invasion assays were performed with the UPEC strains CFT073, originally isolated from the blood of a woman suffering from pyelonephritis, and UTI89, originally isolated from a cystitis patient. We also used control isogenic UTI89ΔFimH, which does not encode the adhesive protein FimH. Each of the UPEC strains exhibited a similar binding capacity to BECs expressing either GFPshRNA or Dyn2shRNA (Fig. 1 B). As predicted, the binding of UTI89ΔFimH was dramatically less than isogenic UTI89 bacteria (Fig. 1 B). Dyn2shRNA markedly reduced the invasion of

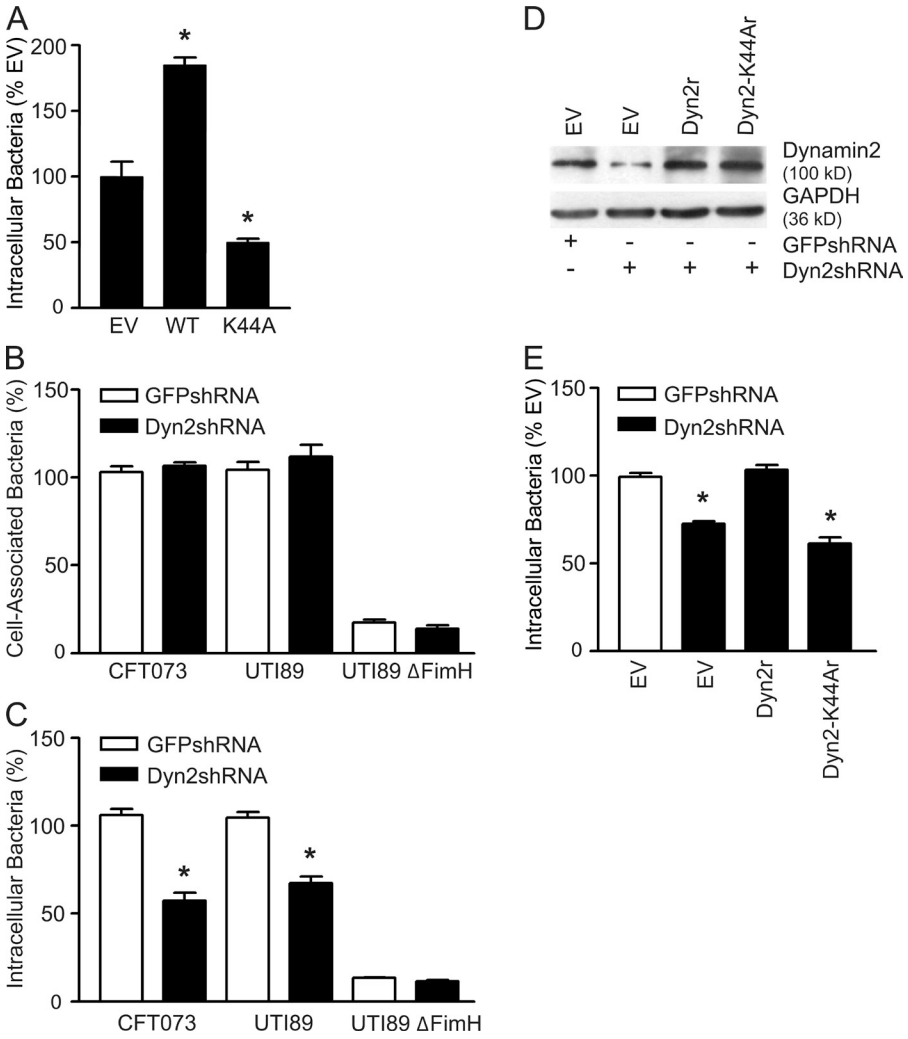

Figure 1. **Dynamin2 regulates the UPEC invasion of BECs.** (A) Forced overexpression of wild-type (WT) dynamin2 significantly increases the type 1 fimbriated *E. coli* ORN103(pSH2) invasion of BECs after 1 h of incubation, whereas the forced overexpression of GTPase-deficient dominant-negative dynamin2 K44A significantly blocks the bacterial entry. Data are expressed relative to control empty vector (EV)–expressing cells. $n = 5$; *, $P < 0.05$ versus empty vector values. (B and C) Bacterial adherence (B) or bacterial invasion (C) after exposure of BECs stably expressing GFPshRNA or Dyn2shRNA to CFT073, UTI89, or UTI89ΔFimH. For CFT073, data are shown relative to GFPshRNA-expressing cells. For UTI89 and UTI89ΔFimH, data are shown relative to GFPshRNA-expressing cells that were incubated with UTI89. $n = 3$; *, $P < 0.05$ versus values from corresponding GFPshRNA-transfected samples. (D) Rescue of shRNA-mediated stable knockdown of endogenous dynamin2 expression with shRNA-resistant wild-type and K44A dynamin2. BECs stably expressing GFPshRNA or Dyn2shRNA were transfected with cDNAs encoding control empty vector or shRNA-resistant wild-type (Dyn2r) or K44A (Dyn2-K44Ar) dynamin2. Cell lysates were analyzed for expression of dynamin2 (top) and GAPDH (bottom) proteins. (E) Re-expression of wild-type, but not K44A, dynamin2 restores bacterial invasion. $n = 3$; *, $P < 0.05$ versus values obtained from GFPshRNA-expressing cells. Data in A–C and E represent means ± SEM.

CFT073 and UTI89 bacteria (Fig. 1 C), providing direct evidence that dynamin2 is a regulator of the UPEC invasion of BECs.

Dynamin2 protein levels in BECs stably infected with lentivirus expressing Dyn2shRNA were restored by a vector expressing either wild-type dynamin2 (Dyn2r) or dominant-negative K44A dynamin2 (Dyn2-K44Ar), each with silent mutations at the shRNA target site (Fig. 1 D). The reintroduction of wild-type dynamin2, but not K44A dynamin2, restored the invasive capacity of UTI89 into host BECs (Fig. 1 E). Together, these results provide evidence that the UPEC invasion of BECs occurs, at least in part, through dynamin2-dependent caveolar portal mobilization from the plasma membrane into the cytosol.

eNOS regulates the UPEC invasion of BECs

In general, bacterial infections cause significant increases in the expression of inducible NOS (iNOS), leading to an increased production of NO (Weng et al., 2009), and NO and its metabolites (e.g., peroxynitrites) exert potent antibacterial effects (Fang, 1997; Chakravortty and Hensel, 2003). The increases in NOS activity and NO production also putatively influence infections of the urinary tract by UPEC, as patients with UTIs have elevated urine concentrations of NO metabolites when compared with healthy subjects (Lundberg et al., 1996; Wheeler et al., 1997). We evaluated the effects of *E. coli* invasion on NO formation in host BECs, which is produced by a NOS-catalyzed conversion of L-arginine to L-citrulline (Hess et al., 2005; Dudzinski et al., 2006). The incubation of BECs with *E. coli* ORN103(pSH2) yielded a time-dependent [^{3}H]L-citrulline accumulation (Fig. S2 A), with marked increases in [^{3}H]L-citrulline levels observed within 30 min of incubation. Exposure of cells to the generic NOS inhibitor L-NAME abolished this effect (Fig. 2 A), demonstrating the specific NOS-dependent NO formation. Unexpectedly, treatment with L-NAME also yielded a dose-dependent decrease in the bacterial invasion of BECs as compared with vehicle-treated cells (Fig. 2 B), suggesting that NOS and NO positively regulate the bacterial uptake.

There are three isoforms of NOS named eNOS, iNOS, and nNOS, and we sought to verify the enzyme involved in the bacteria-regulated increases in NO levels. The *E. coli* ORN103(pSH2)-mediated NO formation was confirmed using the fluorescent NO probe DAF-2DA (Iwakiri et al., 2006), and the results demonstrate rapid (15–30 min) NO accumulation (Fig. S2 B), suggesting eNOS, and not iNOS (Olsson et al., 1998), mediates the NO production during the initial bacterial infection process. In support of this conclusion, bacterial invasion

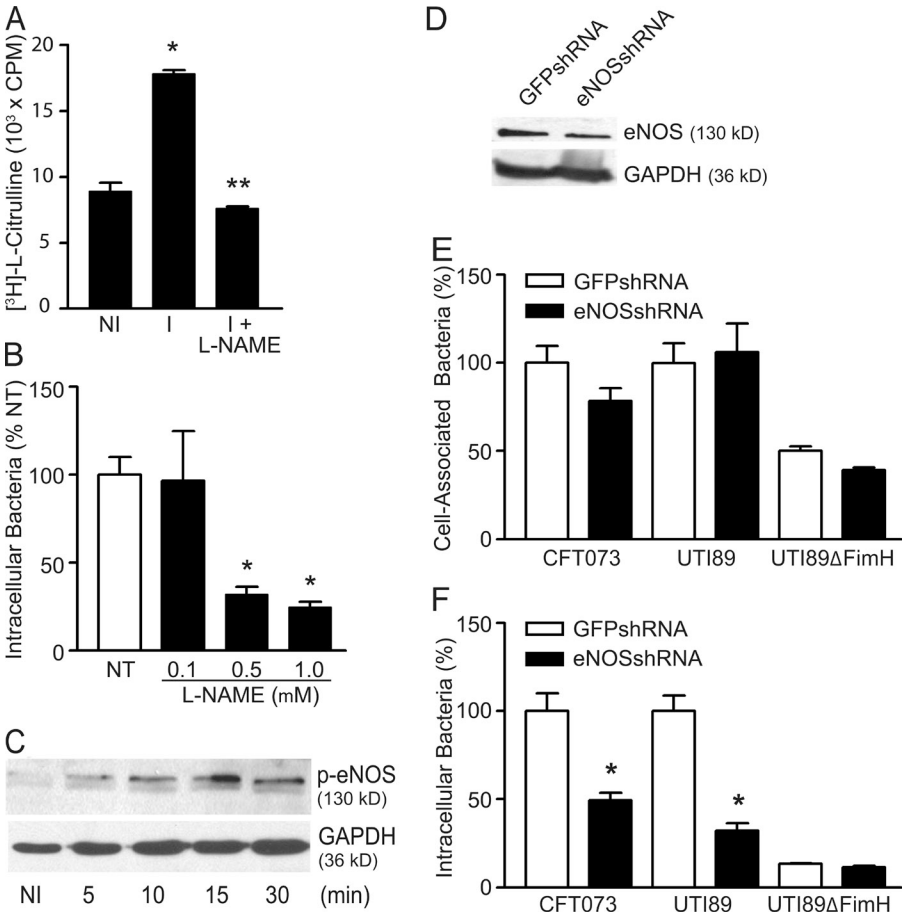

Figure 2. **eNOS regulates the UPEC invasion of BECs.** (A) Enhanced enzymatic activity of eNOS in response to incubation of BECs with *E. coli* ORN103(pSH2), as determined by production of the NOS byproduct L-citrulline. NI, not infected; I, infected; and I + L-NAME, BECs were infected with bacteria in the presence of 100 µM L-NAME. $n = 4$; *, $P < 0.01$ versus uninfected BECs; and **, $P < 0.05$ versus infected BECs. (B) Bacterial invasion after exposure of BECs treated or not treated with escalating doses of L-NAME to *E. coli* ORN103(pSH2). Data are expressed relative to control untreated BECs. $n = 5$; *, $P < 0.05$ versus not treated (NT) cells. (C) Bacterial invasion promotes the rapid phosphorylation of host BEC eNOS. BECs were mixed with *E. coli* ORN103(pSH2) for the indicated times, and equal amounts of cell lysate were analyzed by immunoblotting with anti-phosphoSer1177 eNOS (p-eNOS; top) or anti-GAPDH (bottom) antibodies. (D) BECs infected with adenovirus encoding control GFPshRNA or eNOSshRNA were analyzed by immunoblotting with anti-eNOS (top) or anti-GAPDH (bottom) antibodies. (E and F) Bacterial adherence (E) or bacterial invasion (F) after exposure of BECs stably expressing GFPshRNA or eNOSshRNA to the UPEC strains CFT073, UTI89, or isogenic control UTI89ΔFimH. For CFT073, data are shown relative to GFPshRNA-expressing cells. For UTI89 and UTI89ΔFimH, data are shown relative to GFPshRNA-expressing cells that were incubated with UTI89. $n = 4$; *, $P < 0.01$ versus values from corresponding GFPshRNA-transfected samples. Data represent means ± SEM.

of BECs prompted the rapid phosphorylation of eNOS on S1177 (Fig. 2 C), which was indicative of its activation. To directly implicate eNOS in the bacterial invasion, we suppressed expression of the endogenous eNOS gene using adenovirus-encoded shRNA (eNOSshRNA; Zhang et al., 2006). Western blot analysis of cell lysates showed a >60% reduction in eNOS protein levels by the eNOSshRNA in comparison with GFPshRNA (Fig. 2 D). To establish a role for eNOS in an actual UPEC infection, CFT073, UTI89, and control UTI89ΔFimH clinical UPEC isolates were used in the gentamicin protection assay. No significant differences in the binding ability between eNOSshRNA- and control GFPshRNA-expressing BECs were observed among the UPEC strains (Fig. 2 E). However, the eNOSshRNA significantly attenuated the CFT073 and UTI89 invasion of target BECs but did not further reduce the already low invasion of UTI89ΔFimH (Fig. 2 F). Together, these results show that *E. coli* invasion activates eNOS, which mediates the UPEC invasion of host BECs.

To gain confidence in the contribution of NOS/NO and dynamin2 to UPEC entry into host cells, invasion assays were performed using BECs stably overexpressing dynamin2 or empty vector control in the presence or absence of the NOS inhibitor L-NAME or the NO donor S-nitrosothiol deta-NO. Treatment with L-NAME significantly attenuated the *E. coli* invasion of empty vector–transfected BECs and reversed the dynamin2 overexpression–mediated increases in bacterial invasion (Fig. 3 A). Moreover, treatment with deta-NO significantly increased the *E. coli* invasion of empty vector–transfected BECs but did not impact the already increased bacterial invasion of BECs that overexpress dynamin2 (Fig. 3 A). To confirm that L-NAME and deta-NO do not impact bacterial growth per se, the bacteria were directly exposed to L-NAME or deta-NO followed by determination of colony number. The data (unpublished) demonstrate that treatment with either compound had no significant effect on the *E. coli* growth. Hence, the eNOS- and dynamin2-regulated *E. coli* entry appears to be interrelated in that the dynamin2-mediated increase in invasion was inhibited by L-NAME and was not further increased after treatment with deta-NO (Fig. 3 A). To add confidence to the conclusion that dynamin2 and eNOS collaboratively regulate the UPEC invasion, we targeted the expression of both with shRNA (Fig. S3 A). The reduction of dynamin2 and eNOS expression exhibited little effect on the UPEC binding to BECs (Fig. S3 B). Also, the knockdown of both dynamin2 and eNOS expression attenuated the UPEC invasion by 40–60% (Fig. 3 B), a magnitude similar to the effect of knocking down the individual dynamin2 and eNOS (Fig. S3 C). Together, these findings demonstrate that inhibition of eNOS activity decreases, and elevated NO levels increase, the *E. coli* invasion.

eNOS regulates the UPEC invasion of mouse bladder

To begin to provide a link of our in vitro results (which credibly implicate dynamin2 and eNOS in the UPEC invasion of

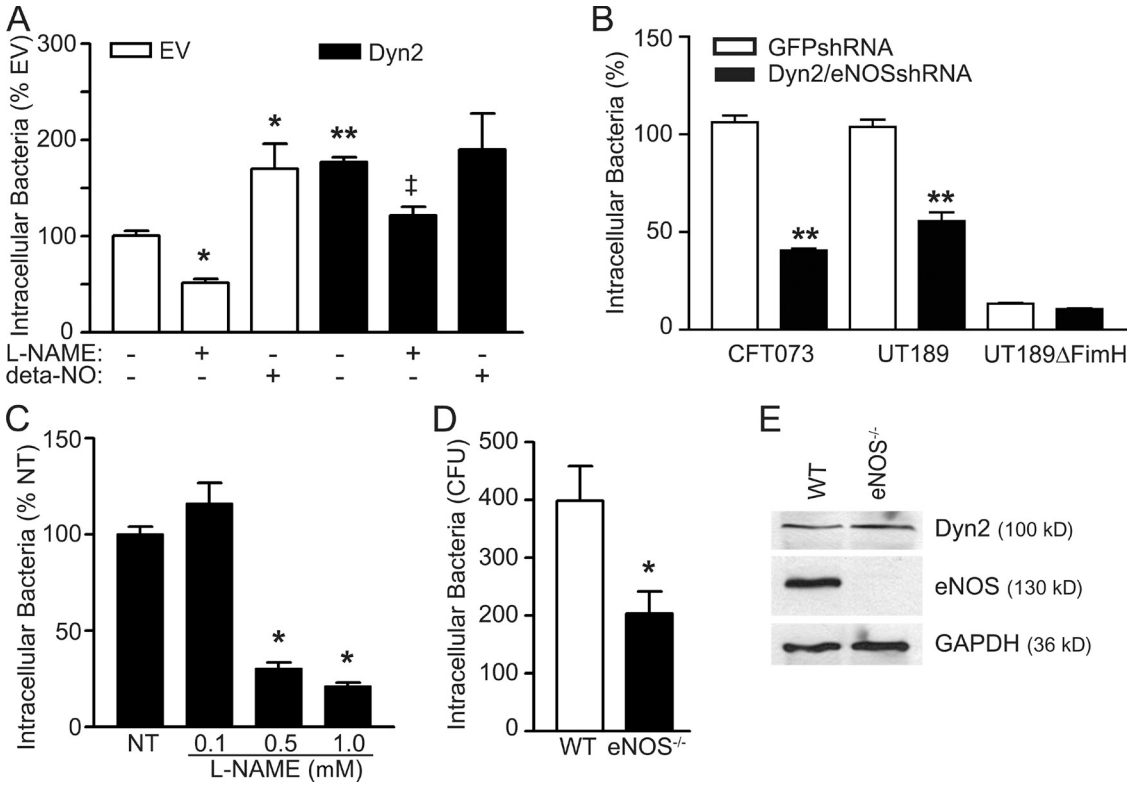

Figure 3. **eNOS controls the UPEC invasion of mouse bladder.** (A) NOS and its product NO regulate the dynamin2-dependent bacterial invasion of BECs. Inhibition of NOS activity with 100 µM L-NAME significantly decreases the *E. coli* ORN103(pSH2) invasion of empty vector (EV)–transfected control BECs (open bars) as well as BECs overexpressing wild-type dynamin2 (shaded bars), and treatment with 500 µM S-nitrosothiol deta-NO increases the bacterial invasion of control (open bars) but not dynamin2-overexpressing BECs (shaded bars). Data shown are for $n = 3$; *, $P < 0.05$ versus untreated control empty vector–expressing BECs; **, $P < 0.01$ versus untreated control empty vector–transfected BECs; and ‡, $P < 0.01$ versus untreated wild-type dynamin2-overexpressing BECs (all by ANOVA). (B) Bacterial invasion after exposure of BECs expressing GFPshRNA or dynamin2shRNA/eNOSshRNA to the UPEC strains CFT073, UTI89, or isogenic control UTI89ΔFimH. For CFT073, data are shown relative to GFPshRNA-expressing cells. For UTI89 and UTI89ΔFimH, data are shown relative to GFPshRNA-expressing cells that were incubated with UTI89. $n = 3$; **, $P < 0.05$ versus values from corresponding GFPshRNA-transfected samples. (C) L-NAME attenuates the bacterial invasion of mouse bladder epithelium. Isolated strips of the bladder transitional epithelium layer were either incubated or not incubated with L-NAME and *E. coli* ORN103(pSH2) for 2 h followed by the determination of bacterial invasion using the gentamicin protection assay. Data for each treatment group were pooled from five animals; *, $P < 0.05$ versus untreated samples by ANOVA (NT, not treated). (D) eNOS$^{-/-}$ bladders exhibit a decreased invasiveness by UPEC. Bladders from eNOS$^{-/-}$ and isogenic control mice were harvested, and transitional epithelium layers were isolated and used for invasion by the UPEC UTI89. Bacterial invasion was assessed by gentamicin protection assay followed by colony counts. $n = 4$; *, $P < 0.01$ versus wild-type (WT) animals. CFU, colony-forming unit. (E) The level of dynamin2 protein expression is not changed in bladder epithelia obtained from eNOS knockout (eNOS$^{-/-}$) compared with wild-type mice. Data in A–D represent means ± SEM.

cultured BECs) to biology, we isolated mouse bladder for use in ex vivo UPEC invasion assays. The mouse bladder was surgically removed and dissected to isolate the transitional epithelium layer, which is the contact site of urine-contained UPEC and the bladder sac. The isolated epithelial tissue was equally dissected into strips, which were individually pretreated or not pretreated with escalating doses of two distinct NOS inhibitors, L-NIO or L-NAME. The tissues were then exposed to *E. coli* and analyzed for bacterial invasion using the gentamicin protection assay. Results demonstrate that treatment with L-NIO (not depicted) or L-NAME (Fig. 3 C) dose-dependently attenuated the bacterial invasion of mouse bladder epithelium.

To further implicate eNOS in the UPEC invasion of mouse bladder, we compared the bacterial uptake in bladders of eNOS$^{-/-}$ and isogenic control littermates using the ex vivo UPEC invasion assay. Results show that UTI89 bacteria invaded eNOS$^{-/-}$ uroepithelia substantially less than uroepithelia from control littermate bladders (Fig. 3 D). Immunoblotting of isolated uroepithelia lysates from eNOS$^{-/-}$ and littermate control animals showed no difference in the expression levels of dynamin2 proteins (Fig. 3 E). Together, these results provide evidence that eNOS, like dynamin2, regulates the UPEC entry into bladder epithelium.

UPEC promote dynamin2 S-nitrosylation

NO activates soluble guanylate cyclase to synthesize cGMP, which, in turn, mediates many of the cellular effects of NO (Hess et al., 2005; Dudzinski et al., 2006). Therefore, we tested the effect of cGMP on *E. coli* ORN103(pSH2) internalization. Exposure of BECs to the cGMP analogue 8-parachlorophenylthio-cGMP did not impact the ability of *E. coli* to internalize (unpublished data), suggesting that alternate NO-regulated mechanisms play a role in the bacterial invasion. Emerging evidence demonstrates that NOSs or chemical NO donors, such as S-nitrosothiols, affect target function by S-nitrosylation of selective proteins (Hess et al., 2005; Dudzinski et al., 2006; Iwakiri et al., 2006), and we have recently demonstrated the S-nitrosylation of ectopically expressed neuronal dynamin1

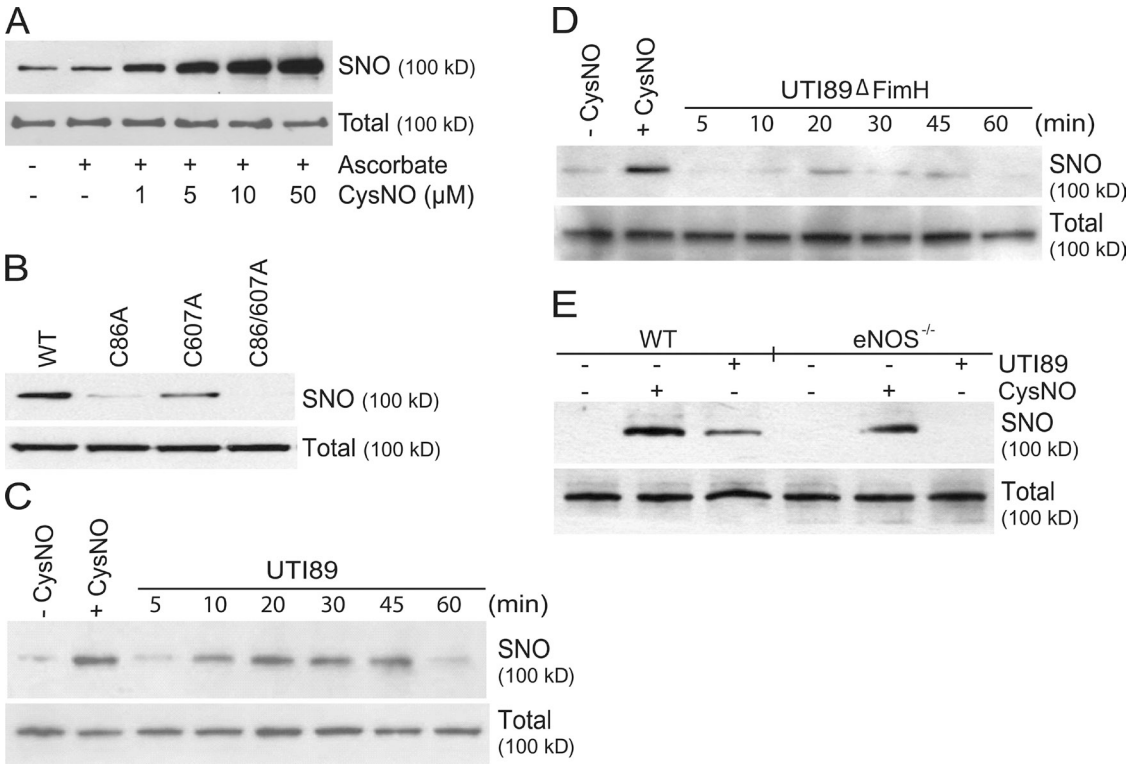

Figure 4. **UPEC invasion promotes the dynamin2 S-nitrosylation at C86 and C607 residues.** (A) S-nitrosylation of HA-tagged wild-type dynamin2 was increased with escalating doses of CysNO, as measured by the biotin-switch method (top). Equal amounts of cell lysate were immunoblotted with anti-HA antibody to show the equal protein loading across all lanes (bottom). (B) S-nitrosylation of dynamin2 is localized to the C86 and C607 residues of dynamin2. BECs were transiently transfected with cDNAs encoding HA-tagged dynamin2 (wild-type [WT], C86A, C607A, or C86/607A) and subjected to S-nitrosylation by 5 μM CysNO as described in A. (C and D) UPEC promote the time-dependent S-nitrosylation of endogenous dynamin2. BECs were incubated with UTI89 (C) or UTI89ΔFimH (D) for the indicated times, and endogenous dynamin2 was subjected to S-nitrosylation analysis using the biotin-switch method. 1 μM CysNO-treated cell extracts was used as a positive control, and total dynamin2 protein is shown on the bottom. (E) UTI89 induces the eNOS-dependent S-nitrosylation of dynamin2 in mouse bladder. Strips of the bladder transitional epithelium layer were harvested from wild-type and isogenic eNOS$^{-/-}$ mice and incubated with UTI89. After 1-h incubation, S-nitrosylation of endogenous dynamin2 was assessed by the biotin-switch method (top). Treatment with CysNO served as a positive control, and total dynamin2 was similar between groups (bottom). SNO, S-nitrosylated protein.

in model HEK293–nNOS cells in a receptor activation–dependent fashion (Wang et al., 2006). Treatment of BECs with the S-nitrosothiol CysNO (Whalen et al., 2007) induced S-nitrosylation of dynamin2 in a dose-dependent manner (Fig. 4 A). To identify sites of nitrosylation, we created dynamin2 forms containing individually mutated cysteine residues and found that S-nitrosylation of dynamin2 is highly localized to C86 residue, as evident by the almost complete lack of S-nitrosylation signal in the dynamin2 C86A form (Fig. 4 B). S-nitrosylation was also observed to occur at residue C607, albeit to lesser levels (Fig. 4 B), and no S-nitrosylation signal could be detected in the dynamin2 protein that contained double C86/607A mutations (Fig. 4 B). These observations are consistent with a study showing the in vitro S-nitrosylation of purified dynamin2 on C86 and C607 (Kang-Decker et al., 2007) but are distinct from those of neuronal dynamin1, which we previously demonstrated is only significantly S-nitrosylated at the C607 residue (Wang et al., 2006).

To determine what, if any, role dynamin2 S-nitrosylation may have in the UPEC invasion, we examined the S-nitrosylation content of endogenous dynamin2 upon incubation of UPEC with BECs. Although a minimal level of endogenous dynamin2 S-nitrosylation could be detected in uninfected BECs, infection with UTI89 caused a significant increase in the dynamin2 S-nitrosylation in a time-dependent manner (Fig. 4 C), suggesting UPEC involvement in the S-nitrosylation of endogenous dynamin2. Notably, the incubation of BECs with noninvasive UTI89ΔFimH bacteria also induced the S-nitrosylation of endogenous dynamin2, albeit considerably less than the parental UTI89 bacteria (Fig. 4 D). To add support to the conclusion that eNOS mediates the UPEC-dependent dynamin2 S-nitrosylation, we analyzed the S-nitrosylation signal in bladder epithelia isolated from eNOS$^{-/-}$ and littermate control mice, which were either subjected or not subjected to UTI89 invasion. Results show that UTI89 promoted the significant S-nitrosylation of dynamin2 in bladder epithelium isolated from wild-type but not eNOS$^{-/-}$ animals (Fig. 4 E).

To examine the locus of the UPEC-mediated dynamin2 S-nitrosylation, BECs expressing individual wild-type, C86A, C607A, or C86/C607A dynamin2 forms were mixed with *E. coli*. As expected, the addition of bacteria to cells in the absence of exogenous NO donors revealed significant S-nitrosylation of wild-type dynamin2 (Fig. 5 A). Distinctly, the *E. coli*–induced S-nitrosylation signal was drastically reduced in dynamin2 C86A and C607A forms (Fig. 5 A), demonstrating that *E. coli* facilitate the dynamin2 S-nitrosylation mainly at the C86 and C607 residues. These results support the conclusion that dynamin2

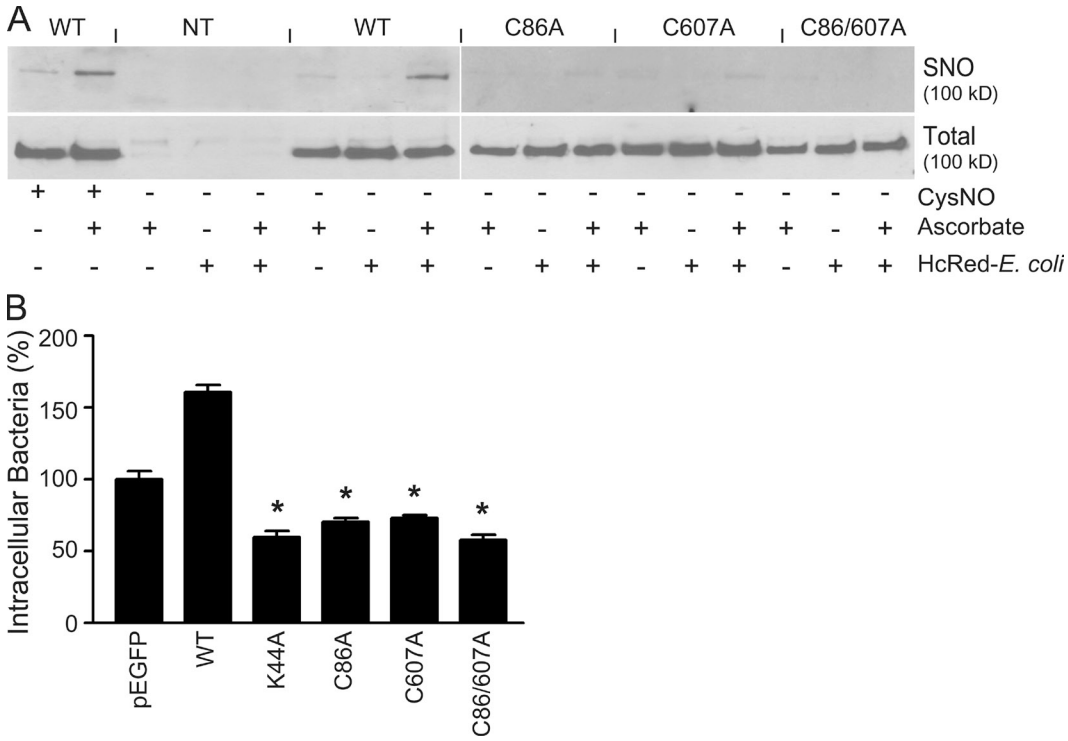

Figure 5. **Requirement of dynamin2 S-nitrosylation on C86 and C607 for *E. coli* entry into BECs.** (A) Bacterial invasion promotes the dynamin2 S-nitrosylation on C86 and C607 residues. BECs were transfected with HA-tagged dynamin2 (wild-type, C86A, C607A, or C86/607A), incubated with type 1 fimbriated HcRed-expressing *E. coli* for 1 h, and subjected to dynamin2 S-nitrosylation analysis by the biotin-switch method. CysNO-treated cell extracts were used as a positive control. NT, not transfected; WT, wild-type dynamin2; and SNO, S-nitrosylated protein. (B) BECs were transiently transfected with cDNAs encoding GFP-dynamin2 (wild type, K44A, C86A, C607A, or C86/607A) fusion proteins and subjected to invasion assays with the HcRed-expressing *E. coli*. Cells were washed, fixed in formalin, and counterstained with DAPI to visualize nuclei. 100 GFP- or GFP-dynamin2–expressing cells from each group were randomly selected, and the number of HcRed-expressing *E. coli* was counted. Each point represents the percent change in intracellular bacteria in comparison with GFP alone–expressing BECs. $n = 3$; *, $P < 0.05$ by ANOVA. Data represent means ± SEM.

is modified by S-nitrosylation at C86 and C607 and that *E. coli* promote this S-nitrosolative event most likely through eNOS activation.

To establish a relationship between dynamin2 S-nitrosylation and *E. coli* entry into host BECs, we examined the effects of GFP-tagged dynamin2 C86A, C607A, or C86/C607A overexpression on bacterial invasion. Results show that forced overexpression of GFP-tagged dynamin2 C86A, C607A, or C86/607A, which are all impaired in nitrosylation, like the dominant-negative dynamin2 K44A, caused a marked decrease in the number of intracellular *E. coli* (Fig. 5 B and Fig. S4). Collectively, these results show that UPEC stimulate eNOS activity, leading to the generation of NO that S-nitrosylates and activates endogenous dynamin2 to facilitate the bacterial invasion of host BECs.

Discussion

UTIs are among the most common bacterial diseases, and a substantial proportion of affected individuals (primarily women) experience recurrent infections (Johnson, 1991; Connell et al., 1996; Foxman et al., 2000; Mulvey et al., 2001). The majority of UTIs are caused by UPEC, and emerging evidence suggests that recurrent UTIs may be caused by intracellular bacteria that manage to evade urinary flushing, immune cell surveillance, and cell membrane–impermeable antibiotics. Hence, elucidating the mechanisms involved in the establishment of intracellular bacteria communities (Anderson et al., 2004) is essential for combating the steady increase in antibiotic resistance and occurrence of recurrent UTIs. Here, we show that UPEC activate host epithelial cell eNOS leading to S-nitrosylation–regulated dynamin2 activation to facilitate the bacterial invasion.

The exact plasma membrane–derived vesicle portals involved in the transport of extracellular UPEC to the inside of BECs remains poorly elucidated, although recent work suggests $Lamp1^+$ endosomes (Mysorekar and Hultgren, 2006), fusiform vesicles (Bishop et al., 2007), and caveolar lipid rafts (Duncan et al., 2004) may be involved. Nonetheless, participant mediators of the fission of these UPEC-containing budding vesicles from the plasma membrane remain incompletely identified even after decades of study, and our findings identified host cell enzymes dynamin2 and eNOS as principal regulators of the bacteria-containing vesicle entry into BECs. The eNOS directly binds dynamin2 (Cao et al., 2001) and may serve as an anchor for dynamin2 stabilization and polymerization at the plasma membrane, thereby allowing dynamin2 to exercise its function of cleaving the bacteria-containing vesicles from the plasma membrane. Indeed, there is an enrichment of HA-dynamin2 proteins at sites of bacterial attachment and entry into host BECs (Fig. S5 A). Hence, UPEC may activate eNOS to promote the assembly-linked activation of dynamin2 on the plasma membrane, thereby allowing establishment of intracellular

UPEC communities (Anderson et al., 2004) that cause recurrent UTIs. In support of this idea, we find that bacterial invasion increases the localization of wild-type, but not nitrosylation-deficient, dynamin2 on the plasma membrane (Fig. S5 B).

Bacterial infections, including the UPEC-acquired UTIs, promote substantial increases in iNOS expression and local NO concentrations, which act as a host cell defense mechanism (Fang, 1997; Wheeler et al., 1997). Our findings are suggestive of an iNOS-independent UPEC invasion into BECs: UPEC entry occurs within minutes of infection, a time frame that is insufficient to markedly alter iNOS protein expression and promotes only a modest, albeit significant, increase in NO levels. Rather, the results are consistent with the idea that eNOS exerts a critical role in the UPEC invasion of BECs: the *E. coli* phosphorylate eNOS on S1177, and knockdown of eNOS expression attenuates UPEC invasion. More to the point, the UPEC invasion of uroepithelia isolated from $eNOS^{-/-}$ mice is significantly less than that of littermate control animals, and, in contrast, it has been reported that $iNOS^{-/-}$ animals exhibit high susceptibility to bacterial infections (Fang, 1997; Chakravortty and Hensel, 2003). Furthermore, iNOS and eNOS are distributed to distinct subcellular compartments, and a recent study showed that protein nitrosylation is confined to the primary site of eNOS localization (Iwakiri et al., 2006). Hence, the source of NO (iNOS vs. eNOS) and amount of NO may dictate the host cell response and fate of the invasive bacteria. Low concentrations of NO, generated by eNOS, act to facilitate bacterial entry, whereas high NO levels, later generated by iNOS, exert nonspecific and bacteriotoxic effects. Indeed, the present results show that uroepithelium from $eNOS^{-/-}$ mice exhibit significantly less UPEC-mediated dynamin2 S-nitrosylation and UPEC invasion. These observations are reminiscent of other biological systems wherein low NO levels act as signal transducers involved in the normal cellular physiology and high levels of NO exert pathophysiologic effects (Pervin et al., 2007; Thomas et al., 2008).

The present study shows that UPEC promote eNOS activation and dynamin2 S-nitrosylation at conserved C86 and C607 residues and that dynamin2 S-nitrosylation appears to be critical for the UPEC entry into BECs. A remaining question is how UPEC activate host epithelial cell eNOS and dynamin2. Bacterial binding to host cell plasma membrane–anchored receptors is a required first step in the invasion process (Krogfelt et al., 1990; Connell et al., 1996). Treatment with methyl-α-D-mannose, which interferes with the association of UPEC with host cell glycoproteins, showed no effect on the UPEC-mediated NO production (unpublished data), suggesting a possible existence of soluble bacteria factors that activate eNOS. Indeed, eNOS undergoes phosphorylation-dependent activation in response to a diverse array of extracellular signals that converge to activate intracellular kinases, including Akt and the cAMP-dependent protein kinase PKA (Michell et al., 2001). Our results show that UTI89ΔFimH, like parental UTI89, is capable of promoting the cAMP accumulation (unpublished data) as well as dynamin2 S-nitrosylation, leading us to propose that a soluble UPEC factor may initiate a cAMP→PKA→eNOS→dynamin2 activation signaling cascade, which is required for the UPEC invasion. Identification of dynamin2 S-nitrosylation and eNOS-specific inhibitors may provide a clinical benefit to more effectively treat recurrent UTIs, which disproportionately affect women and are currently incurable.

Materials and methods

DNA reagents

Complementary DNAs encoding wild-type and K44A dynamin2 were previously described (Ahn et al., 1999; Wang et al., 2006). Mutations of dynamin2 were created with a site-directed mutagenesis kit (QuikChange; Agilent Technologies) using the primers C86A sense, 5′-GAGTTTTTGCACGCTAAGTCCAAAAAGTTT-3′; C86A antisense, 5′-AAACTTTTTGGACTTAGCGTGCAAAAACTC-3′; C607A sense, 5′-ATCGAACTGGCTGCTGACTCCCAGGAA-3′; and C607A antisense, 5′-TTCCTGGGAGTCAGCAGCCAGTTCGAT-3′.

Knockdown and rescue of dynamin2 in BECs

Lentiviral DNA expression vectors were purchased from Thermo Fisher Scientific. Each expression vector contained 21-nt shRNA duplexes targeting dynamin2: 5′-GCAGTCGTACATCAACACAAA-3′, 5′-GCCGGAACATTGAACATTTAA-3′, and 5′-CCTTGAAGAATGTGTCCTGAT-3′. 3 µg of each expression vector was cotransfected with equal concentrations of vesicular stomatitis virus G and the Δ8.9 vector into 293T cells using transfection reagent (FuGENE 6; Roche). As a negative control, 293T cells were transfected with the same amount of expression vector containing a GFP-targeting sequence (5′-GCAAGCTGACCCTGAAGTTCAT-3′). After 24 h, the medium from transfected 293T cells was collected, mixed with 5 µl polybrene, and added to the BECs. New medium was added to the 293T cells for an additional 24 h, and the BECs were infected a second time. The duration of viral infection of the BECs was 2 h, and then the medium was changed to RPMI 1640 containing 10% FBS. After 48 h, the shRNA-expressing cells were selected with 2 µg/ml puromycin. Plates of BECs not infected with virus were used in parallel treatment with puromycin as a selection control. When the uninfected control cells were completely killed, the infected cell medium was replaced with complete medium containing 1 µg/ml puromycin for maintenance. The level of protein was determined by immunoblotting using dynamin2-specific antibody. Knockdown-resistant dynamin2 was made with the site-directed mutagenesis kit (QuikChange) without changing the coding amino acids (5′-GCAGTCCTACATCAACACGAA-3′).

Knockdown of eNOS expression in BECs

Adenoviruses encoding shRNA that target human eNOS sequences (gift from D. Fulton, Medical College of Georgia, Augusta, GA) were used to infect BECs (Zhang et al., 2006). Cells were harvested after 36 h of infection, and lysates were used to confirm the decreased expression of eNOS protein by immunoblot analysis.

Bacteria strains and cell culture

The laboratory isolate *E. coli* K-12 derivative ORN103(pSH2), containing a deletion of the type 1 fimbrial gene cluster and transformed with plasmid pSH2, which encodes type 1 fimbrial gene clusters plus a chloramphenicol resistance marker, *E. coli* ORN103(pSH2) expressing pHcRed (gift from S. Abraham, Duke University, Durham, NC; Duncan et al., 2004), and three clinical strains, UTI89, UTI89ΔFimH, and CFT073 (gift from M. Mulvey, University of Utah, Salt Lake City, UT), were used at an MOI of 10–50. The human bladder epithelial cancer cell line 5637 (BEC) was obtained from American Type Culture Collection (HTB-9) and was cultured in RPMI 1640 medium supplemented with 10% FBS without antibiotics at 37°C in a humidified atmosphere of 5% CO_2. Cells were transfected using the appropriate cDNAs and Lipofectamine (Invitrogen), and experiments were performed 1 d after transfection.

Bacteria cell association and invasion assays

BECs were seeded at 5×10^4 cells per well in 96-well plates and allowed to grow to confluence. Cells were serum starved overnight in culture medium containing 10 mM Hepes, pH 7.5, and 0.1% BSA and infected upon addition of the indicated bacteria strain for 1 h at 37°C. For bacterial cell association measurement, BECs were collected by centrifugation, washed four times with PBS, and lysed in PBS containing 0.25% (volume per volume) Triton X-100. Dilutions (1:10 and 1:100) of lysates were plated on Luria broth agar plates with chloramphenicol, and colonies were allowed to grow and counted the next day. To determine the number of internalized bacteria, cell culture medium containing infecting bacteria was replaced with fresh medium containing 100 µg/ml of membrane-impermeable

gentamicin antibiotic (to kill extracellular bacteria). After 30–60 min, cells were washed four times in PBS, lysed, and plated (1:10 and 1:100 dilutions) on Luria broth agar plates for colony counting, and, on average, the colony numbers ranged from 100 to 400.

For determining the effect of dynamin2 S-nitrosylation on UPEC invasion, BECs were transiently transfected with cDNAs encoding GFP-dynamin2 fusion proteins, seeded onto glass coverslips, and infected with HcRed-expressing *E. coli*. Cells were washed and treated with gentamicin (to kill extracellular bacteria) as described in the previous paragraph. Cells were fixed in 10% formalin solution and stained with DAPI to visualize nuclei. For each experiment, internalized bacteria were analyzed from 100 randomly selected GFP-dynamin2–expressing cells. Cells expressing HA-dynamin2 were stained with an anti-HA antibody followed by an Alexa Fluor 488–conjugated secondary antibody, and cells expressing GFP-dynamin2 and invaded with HcRed bacteria were visualized using microscopy. In brief, cells were mounted using fluorescence mounting medium (Dako) and were examined using a confocal microscope (TCS SP5; Leica) equipped with a 40×/1.25 NA oil immersion lens. Images were captured and analyzed using the application suite advanced fluorescence 2.0.2 software (Leica).

For animal studies, bladders were harvested from 5–7-wk-old female C57BL/6 mice and macrodissected to isolate the transitional epithelium layer. Tissues were cut into strips and placed in RPMI 1640 medium for infection with UPEC. To inhibit NOS activity, tissues were treated with L-NAME or L-NIO before mixing with the UPEC. Bladder tissues were then washed twice with gentamicin solution and incubated for an additional 30 min to allow complete killing of floating and unincorporated bacteria. Bladder tissues were minced, lysed, and subjected to the colony formation assay. In all cases, levels of cell-associated or intracellular bacteria are expressed relative to control samples. All assays were repeated at least three times in triplicate, and significant differences between controls and experimental samples were determined by analysis of variance (ANOVA; with $P < 0.05$ considered to be significant).

Immunoblotting

Total and phosphorylated protein levels were detected by immunoblotting. Cells were lysed in radio immunoprecipitation assay buffer (Wang et al., 2006; Whalen et al., 2007), and whole cell lysates were subjected to protein quantification using the Bradford method. Equal amounts of protein were resolved by SDS-PAGE, transferred to nitrocellulose membranes, and immunoblotted with dynamin2 (1:1,000 dilution; Cell Signaling Technology), phosphoSer1177-eNOS (1:500 dilution; Transduction Laboratories), total eNOS (1:500 dilution; Transduction Laboratories), glyceraldehyde 3-phosphate dehydrogenase (GAPDH; 1:5,000 dilution; Millipore), or HA (1:5,000 dilution; Abcam) antibodies. Filters were incubated with the appropriate HRP-conjugated secondary antibody and developed with enzyme-linked chemiluminescence.

NOS activation assay

The enzymatic activity of NOS was assessed as the formation of [^{3}H]L-citrulline from the radiolabeled NOS substrate [^{3}H]L-arginine. BECs were incubated with *E. coli* ORN103(pSH2) in the presence of 3–5 µCi/ml [^{3}H]L-arginine (41 Ci/mmol; PerkinElmer) in a buffer containing 25 mM Hepes, pH 7.3, 100 mM NaCl, 5.4 mM KCl, 1 mM $CaCl_2$, 1 mM $MgSO_4$, 25 mM glucose, and 10 µM of unlabeled L-arginine. After the indicated incubation times, cells were washed with PBS, scraped into stop solution containing 20 mM sodium acetate, 1 mM L-citrulline, 2 mM EDTA, and 2 mM EGTA, pH 5.5, and homogenized. An aliquot of the protein sample was preserved for the determination of protein content, and the remaining cell lysate was added to a column (Dowex 50W-X8 400; Bio-Rad Laboratories) to separate [^{3}H]L-citrulline. The flow-through fraction was analyzed by liquid scintillation counting. In addition to infected cells, each experimental condition included uninfected cells and samples of *E. coli* ORN103(pSH2) alone to account for basal BECs and *E. coli* [^{3}H]L-citrulline formation, respectively. For NOS inhibition experiments, cells were pretreated with 100 µM L-NAME overnight before the addition of [^{3}H]L-arginine.

Protein S-nitrosylation

Appropriately treated BECs or isolated mouse bladder transitional epithelia were lysed in 400 µl of lysis buffer (25 mM Hepes, pH 7.7, 50 mM NaCl, 1 mM EDTA, 0.1 mM neocuproine, 1% NP-40, and protease inhibitor cocktail [Complete; Roche]). Cell/tissue extracts were diluted to 1 ml with HEN buffer (250 mM Hepes, 1 mM EDTA, and 0.1 mM neocuproine, pH 7.7), and detection of dynamin2 S-nitrosylation was performed using the biotin-switch method as we previously described (Wang et al., 2006; Whalen et al., 2007).

Statistical analysis

The significance of the treatment-induced cellular response was analyzed by two-way ANOVA with Bonferroni posttest and implied at $P < 0.05$. All statistical analyses were performed, and all graphs generated, using Prism 5.0 software (GraphPad Software, Inc.). The x and y labels of all presented data were prepared using the Illustrator suite (CS2; Adobe).

Online supplemental material

Fig. S1 shows the role of caveolae and dynamin in bacterial invasion. Fig. S2 shows the bacteria-mediated increase in NO formation. Fig. S3 shows the effect of knocking down the expression of dynamin2 and eNOS on bacteria invasion. Fig. S4 shows the requirement of dynamin2 S-nitrosylation for bacteria invasion. Fig. S5 shows the effect of bacteria invasion on the subcellular distribution of dynamin2. Online supplemental material is available at http://www.jcb.org/cgi/content/full/jcb.201003027/DC1.

We thank Drs. D. Fulton, M. Mulvey, and S.N. Abraham for sharing reagents and technical advice and J.I. Kim and J.S. Stamler for helpful discussion.

This work was supported by the National Institutes of Health grants AI65927 and AI079014 to Y. Daaka. Z. Wang, Z. Nie, N.H. Moniri, and Y. Daaka designed the experiments. Z. Wang, C. Humphrey, N. Frilot, G. Wang, Z. Nie, and N.H. Moniri performed the experiments in this work. Z. Wang, N.H. Moniri, and Y. Daaka wrote the paper. The other authors read and commented on the manuscript.

Submitted: 5 March 2010
Accepted: 7 December 2010

References

Achiriloaie, M., B. Barylko, and J.P. Albanesi. 1999. Essential role of the dynamin pleckstrin homology domain in receptor-mediated endocytosis. *Mol. Cell. Biol.* 19:1410–1415.

Ahn, S., S. Maudsley, L.M. Luttrell, R.J. Lefkowitz, and Y. Daaka. 1999. Src-mediated tyrosine phosphorylation of dynamin is required for β2-adrenergic receptor internalization and mitogen-activated protein kinase signaling. *J. Biol. Chem.* 274:1185–1188. doi:10.1074/jbc.274.3.1185

Anderson, G.G., S.M. Martin, and S.J. Hultgren. 2004. Host subversion by formation of intracellular bacterial communities in the urinary tract. *Microbes Infect.* 6:1094–1101. doi:10.1016/j.micinf.2004.05.023

Bishop, B.L., M.J. Duncan, J. Song, G.J. Li, D. Zaas, and S.N. Abraham. 2007. Cyclic AMP-regulated exocytosis of *Escherichia coli* from infected bladder epithelial cells. *Nat. Med.* 13:625–630. doi:10.1038/nm1572

Cao, S., J. Yao, T.J. McCabe, Q. Yao, Z.S. Katusic, W.C. Sessa, and V. Shah. 2001. Direct interaction between endothelial nitric-oxide synthase and dynamin-2. Implications for nitric-oxide synthase function. *J. Biol. Chem.* 276:14249–14256.

Chakravortty, D., and M. Hensel. 2003. Inducible nitric oxide synthase and control of intracellular bacterial pathogens. *Microbes Infect.* 5:621–627. doi:10.1016/S1286-4579(03)00096-0

Connell, I., W. Agace, P. Klemm, M. Schembri, S. Mărild, and C. Svanborg. 1996. Type 1 fimbrial expression enhances *Escherichia coli* virulence for the urinary tract. *Proc. Natl. Acad. Sci. USA.* 93:9827–9832. doi:10.1073/pnas.93.18.9827

Conner, S.D., and S.L. Schmid. 2003. Regulated portals of entry into the cell. *Nature.* 422:37–44. doi:10.1038/nature01451

Dhakal, B.K., R.R. Kulesus, and M.A. Mulvey. 2008. Mechanisms and consequences of bladder cell invasion by uropathogenic *Escherichia coli*. *Eur. J. Clin. Invest.* 38(Suppl. 2):2–11. doi:10.1111/j.1365-2362.2008.01986.x

Doherty, G.J., and H.T. McMahon. 2009. Mechanisms of endocytosis. *Annu. Rev. Biochem.* 78:857–902. doi:10.1146/annurev.biochem.78.081307.110540

Dudzinski, D.M., J. Igarashi, D. Greif, and T. Michel. 2006. The regulation and pharmacology of endothelial nitric oxide synthase. *Annu. Rev. Pharmacol. Toxicol.* 46:235–276. doi:10.1146/annurev.pharmtox.44.101802.121844

Duncan, M.J., G.J. Li, J.S. Shin, J.L. Carson, and S.N. Abraham. 2004. Bacterial penetration of bladder epithelium through lipid rafts. *J. Biol. Chem.* 279:18944–18951. doi:10.1074/jbc.M400769200

Eto, D.S., H.B. Gordon, B.K. Dhakal, T.A. Jones, and M.A. Mulvey. 2008. Clathrin, AP-2, and the NPXY-binding subset of alternate endocytic adaptors facilitate FimH-mediated bacterial invasion of host cells. *Cell. Microbiol.* 10:2553–2567. doi:10.1111/j.1462-5822.2008.01229.x

Fang, F.C. 1997. Mechanisms of nitric oxide-related antimicrobial activity. *J. Clin. Invest.* 100:S43–S50.

Foxman, B., R. Barlow, H. D'Arcy, B. Gillespie, and J.D. Sobel. 2000. Urinary tract infection: self-reported incidence and associated costs. *Ann. Epidemiol.* 10:509–515. doi:10.1016/S1047-2797(00)00072-7

Francis, C.L., T.A. Ryan, B.D. Jones, S.J. Smith, and S. Falkow. 1993. Ruffles induced by *Salmonella* and other stimuli direct macropinocytosis of bacteria. *Nature.* 364:639–642. doi:10.1038/364639a0

Hess, D.T., A. Matsumoto, S.O. Kim, H.E. Marshall, and J.S. Stamler. 2005. Protein S-nitrosylation: purview and parameters. *Nat. Rev. Mol. Cell Biol.* 6:150–166. doi:10.1038/nrm1569

Iwakiri, Y., A. Satoh, S. Chatterjee, D.K. Toomre, C.M. Chalouni, D. Fulton, R.J. Groszmann, V.H. Shah, and W.C. Sessa. 2006. Nitric oxide synthase generates nitric oxide locally to regulate compartmentalized protein S-nitrosylation and protein trafficking. *Proc. Natl. Acad. Sci. USA.* 103:19777–19782. doi:10.1073/pnas.0605907103

Johnson, J.R. 1991. Virulence factors in *Escherichia coli* urinary tract infection. *Clin. Microbiol. Rev.* 4:80–128.

Kang-Decker, N., S. Cao, S. Chatterjee, J. Yao, L.J. Egan, D. Semela, D. Mukhopadhyay, and V. Shah. 2007. Nitric oxide promotes endothelial cell survival signaling through S-nitrosylation and activation of dynamin-2. *J. Cell Sci.* 120:492–501. doi:10.1242/jcs.03361

Krogfelt, K.A., H. Bergmans, and P. Klemm. 1990. Direct evidence that the FimH protein is the mannose-specific adhesin of *Escherichia coli* type 1 fimbriae. *Infect. Immun.* 58:1995–1998.

Lundberg, J.O.N., I. Ehrén, O. Jansson, J. Adolfsson, J.M. Lundberg, E. Weitzberg, K. Alving, and N.P. Wiklund. 1996. Elevated nitric oxide in the urinary bladder in infectious and noninfectious cystitis. *Urology.* 48:700–702. doi:10.1016/S0090-4295(96)00423-2

Mettlen, M., T. Pucadyil, R. Ramachandran, and S.L. Schmid. 2009. Dissecting dynamin's role in clathrin-mediated endocytosis. *Biochem. Soc. Trans.* 37:1022–1026. doi:10.1042/BST0371022

Michell, B.J., T. Chen Zp, T. Tiganis, D. Stapleton, F. Katsis, D.A. Power, A.T. Sim, and B.E. Kemp. 2001. Coordinated control of endothelial nitric-oxide synthase phosphorylation by protein kinase C and the cAMP-dependent protein kinase. *J. Biol. Chem.* 276:17625–17628. doi:10.1074/jbc.C100122200

Miyauchi, K., Y. Kim, O. Latinovic, V. Morozov, and G.B. Melikyan. 2009. HIV enters cells via endocytosis and dynamin-dependent fusion with endosomes. *Cell.* 137:433–444. doi:10.1016/j.cell.2009.02.046

Mulvey, M.A. 2002. Adhesion and entry of uropathogenic *Escherichia coli*. *Cell. Microbiol.* 4:257–271. doi:10.1046/j.1462-5822.2002.00193.x

Mulvey, M.A., J.D. Schilling, and S.J. Hultgren. 2001. Establishment of a persistent *Escherichia coli* reservoir during the acute phase of a bladder infection. *Infect. Immun.* 69:4572–4579. doi:10.1128/IAI.69.7.4572-4579.2001

Mysorekar, I.U., and S.J. Hultgren. 2006. Mechanisms of uropathogenic *Escherichia coli* persistence and eradication from the urinary tract. *Proc. Natl. Acad. Sci. USA.* 103:14170–14175. doi:10.1073/pnas.0602136103

Olsson, L.E., M.A. Wheeler, W.C. Sessa, and R.M. Weiss. 1998. Bladder instillation and intraperitoneal injection of *Escherichia coli* lipopolysaccharide up-regulate cytokines and iNOS in rat urinary bladder. *J. Pharmacol. Exp. Ther.* 284:1203–1208.

Pervin, S., R. Singh, E. Hernandez, G.Y. Wu, and G. Chaudhuri. 2007. Nitric oxide in physiologic concentrations targets the translational machinery to increase the proliferation of human breast cancer cells: involvement of mammalian target of rapamycin/eIF4E pathway. *Cancer Res.* 67:289–299. doi:10.1158/0008-5472.CAN-05-4623

Pizarro-Cerdá, J., and P. Cossart. 2006. Bacterial adhesion and entry into host cells. *Cell.* 124:715–727. doi:10.1016/j.cell.2006.02.012

Pizzato, M., A. Helander, E. Popova, A. Calistri, A. Zamborlini, G. Palù, and H.G. Göttlinger. 2007. Dynamin 2 is required for the enhancement of HIV-1 infectivity by Nef. *Proc. Natl. Acad. Sci. USA.* 104:6812–6817. doi:10.1073/pnas.0607622104

Thomas, D.D., L.A. Ridnour, J.S. Isenberg, W. Flores-Santana, C.H. Switzer, S. Donzelli, P. Hussain, C. Vecoli, N. Paolocci, S. Ambs, et al. 2008. The chemical biology of nitric oxide: implications in cellular signaling. *Free Radic. Biol. Med.* 45:18–31. doi:10.1016/j.freeradbiomed.2008.03.020

Veiga, E., J.A. Guttman, M. Bonazzi, E. Boucrot, A. Toledo-Arana, A.E. Lin, J. Enninga, J. Pizarro-Cerdá, B.B. Finlay, T. Kirchhausen, and P. Cossart. 2007. Invasive and adherent bacterial pathogens co-Opt host clathrin for infection. *Cell Host Microbe.* 2:340–351. doi:10.1016/j.chom.2007.10.001

Wang, G.F., N.H. Moniri, K. Ozawa, J.S. Stamler, and Y. Daaka. 2006. Nitric oxide regulates endocytosis by S-nitrosylation of dynamin. *Proc. Natl. Acad. Sci. USA.* 103:1295–1300. doi:10.1073/pnas.0508354103

Weng, T.I., H.Y. Wu, P.Y. Lin, and S.H. Liu. 2009. Uropathogenic *Escherichia coli*-induced inflammation alters mouse urinary bladder contraction via an interleukin-6-activated inducible nitric oxide synthase-related pathway. *Infect. Immun.* 77:3312–3319. doi:10.1128/IAI.00013-09

Whalen, E.J., M.W. Foster, A. Matsumoto, K. Ozawa, J.D. Violin, L.G. Que, C.D. Nelson, M. Benhar, J.R. Keys, H.A. Rockman, et al. 2007. Regulation of β-adrenergic receptor signaling by S-nitrosylation of G-protein-coupled receptor kinase 2. *Cell.* 129:511–522. doi:10.1016/j.cell.2007.02.046

Wheeler, M.A., S.D. Smith, G. García-Cardeña, C.F. Nathan, R.M. Weiss, and W.C. Sessa. 1997. Bacterial infection induces nitric oxide synthase in human neutrophils. *J. Clin. Invest.* 99:110–116. doi:10.1172/JCI119121

Zhang, Q., J.E. Church, D. Jagnandan, J.D. Catravas, W.C. Sessa, and D. Fulton. 2006. Functional relevance of Golgi- and plasma membrane-localized endothelial NO synthase in reconstituted endothelial cells. *Arterioscler. Thromb. Vasc. Biol.* 26:1015–1021. doi:10.1161/01.ATV.0000216044.49494.c4